Copyright © 1998, by the International Council of the Aeronautical Sciences (ICAS)
and the American Institute of Aeronautics and Astronautics, Inc.

ICAS-98-3,10,2

A98-31568

# BEHAVIOURS OF SEPARATED AND REATTACHING FLOW FORMED OVER BACKWARD FACING STEP

Kenichi RINOIE*, Yasuhiro SHIRAI†, Yoshihiro SAITO†
and Yasuto SUNADA‡
University of Tokyo, Tokyo 113-8656, Japan

## Abstract

Wind tunnel measurements were done for the separated and reattaching flow formed over backward facing step. Turbulent energy and turbulent normal stress balances were estimated from the measured data of mean velocities, Reynolds stresses and turbulent triple products. The main objective of the experiments is to analyze the turbulent structure inside the reattaching shear layer, including the reverse flow, in detail. The results indicated different turbulent structures in three classified regions of the backward facing step flow, i.e. the dead air, reverse flow and separated shear layer regions. In the reverse flow region, the transverse diffusion by turbulence in the turbulent energy balance equation is positive. The production term by shear stress, the transverse diffusion term by turbulence, and the advection term similarly help to balance the dissipation term in the same region. Classified Reynolds stress that are $u$ positive and $v$ negative contribute the most to the generation of Reynolds shear stress in this region.

## Nomenclature

$Cp$ surface pressure coefficient
$h$ step height, m
$k$ turbulent kinetic energy, $m^2/s^2$
$p$ pressure fluctuation, $N/m^2$
$R$ reverse flow rate
$u, v, w$ components of fluctuating velocity along the $x$-, $y$- and spanwise directions, m/s
$\overline{uv_c}$ classified Reynolds shear stress, $m^2/s^2$
$U, V$ components of instantaneous velocity along $x$-, $y$-directions, m/s
$U_\infty$ free stream velocity at $x$=0, m/s
$x$ Cartesian coordinate along the free stream direction measured from the step, m
$x_R$ $x$ coordinate of the reattachment point, m
$y$ Cartesian coordinate perpendicular to and measured from the surface of the model, m
$\delta_\omega$ maximum slope thickness, m
$\varepsilon$ rate of dissipation of turbulent kinetic energy, $m^2/s^3$
$\varepsilon_u$ rate of dissipation of longitudinal Reynolds normal stress ($\overline{u^2}$), $m^2/s^3$
$\varepsilon_v$ rate of dissipation of transverse Reynolds normal stress ($\overline{v^2}$), $m^2/s^3$
$\rho$ air density, $kg/m^3$
$\psi$ stream function, $m^2/s$

## 1. Introduction

Separated and reattaching flows formed around bodies such as aerofoils and vehicles often significantly affect their aerodynamic characteristics. The flow that is formed over the backward facing step is one of the simplest forms of separated and reattaching flows. The flow separates at the step, develops as a separated shear layer, and reattaches to the wall (Fig.1). The separation point is fixed at the step position. The streamline just after the separation is parallel to the direction of the main stream. When the boundary layer upstream of the step is laminar, the transition occurs just after the separation because of the instability of the separated shear layer, when the Reynolds number of the flow is moderately high. The flow around the reattaching region is generally governed by turbulent phenomenon, regardless of the flow conditions at the step, (i.e. laminar or turbulent).

Numerous studies have been done in regard to the backward facing step flow[1-9]. One of its features

* Associate Professor, Department of Aeronautics and Astronautics, 7-3-1 Hongo, Bunkyo-ku .
† Graduate Student, ‡ Research Assistant



21st ICAS Congress
13-18 September 1998
Melbourne, Australia

Copyright © 1998 by ICAS and AIAA. All rights reserved

Copyright © 1998, by the International Council of the Aeronautical Sciences (ICAS)
and the American Institute of Aeronautics and Astronautics, Inc.

is the complexity of turbulent structures. The flow just downstream of the step has a similar flow structure to the plain mixing layer[2]. However, the reverse flow (recirculating) region that is upstream from the reattachment point is governed by the non-equilibrium behaviour of turbulence[5], i.e. the turbulent energy production and the dissipation do not balance. Another one of its features is that the separated shear layer exhibits unsteadiness due to the vortical structure[2] that is formed at the step. This structure moves along the streamline and collides with the surface at the reattachment point. Due to this vortical structure, the reattachment point moves upstream and downstream at a very low frequency, i.e. this is known as "flapping"[4].

Turbulent energy balance is a methodology that can assist in understanding the turbulent flow structure of the backward facing step[3,5,8,9]. The turbulent energy production term and the dissipation term are dominant inside the separated shear layer[3]. The turbulent diffusion term also attributes to the development of turbulent energy[5,8]. Even after the reattachment, the turbulent diffusion term plays an important role near the wall[9]. However, in order to clarify the turbulent structure inside the separated flow (including the reverse flow region), more detailed measurements and analysis of the backward step flow is necessary.

Many numerical simulations for the backward facing step flow have also been done[10-12]. Most of these incorporated a two equation k-ε turbulence model for the simulations. It has been found that the present k-ε turbulence model does not properly simulate the separated region with a reverse flow, because this turbulence model assumes the existence of a locally equilibrium turbulent structure, together with an eddy viscosity hypothesis and a gradient diffusion model[5]. The turbulent flows inside the separated region, especially the recirculating region, should be measured and discussed in detail in order to create a more sophisticated turbulence model.

Morinishi and Kobayashi[13] discussed the turbulent structure inside the separated region by using results obtained by a large eddy simulation method. They showed that the turbulent structure of the backward facing step flow could be classified into four regions depending on the numerically estimated Reynolds stress balances. However, a classification system for the turbulent structure that is based on measured data has not been discussed in detail.

In this study, wind tunnel measurements were done for the backward facing step flow. The boundary layer upstream from the step is turbulent. The mean velocities, Reynolds stresses, and turbulent triple products were measured by two-component laser Doppler velocimetry. The Reynolds number which is based on the height of step was $2 \times 10^4$. The turbulent energy and turbulent normal stress balances were estimated. The turbulent structures inside the separated and reverse flow region are discussed.

In summary, the purpose of this study is to clarify the turbulent behaviour of the backward facing step flow, (especially inside the reattaching shear layer and including the reverse flow), using a turbulent energy balance.

## 2. Experimental Details

Measurements were done in a low speed suction type wind tunnel that has a test section 600mm in height, 200mm in width and 1000mm in length[14]. Tunnel speed was set so that the free stream velocity at the step, $U_\infty$, was 15m/s. The freestream turbulence intensity of the tunnel is less than 0.16%. Figure 2 shows the backward facing step model. The distance between the leading-edge of the model and its step is 250mm. Step height $h$ is 0.02m. The aspect ratio (i.e. the tunnel width ratio vs. step height) is 10. A surface oil flow visualisation test was made in order to confirm the two dimensionality of the mean flow at the tunnel centre line. The vertical distance between the upper wall of the tunnel and the surface of the model downstream of the step is 300mm, i.e. the transverse expansion ratio is 1.07. A 2.4mm diameter coil spring was attached on the surface of the model 25mm downstream from the leading-edge of the model so that the boundary layer just upstream from the step is completely turbulent. Mean longitudinal velocity distributions $\overline{U}/U_\infty$ at $x/h$=-0.5 closely follow the universal logarithmic curve, with a skin friction coefficient value of 0.0042 giving the best fit. The momentum thickness at this point is 1.22mm.

On the upper surface of the model, 19 pressure holes are located at 20mm spanwise position from the centre line of the tunnel. The surface pressure measurements were made with a pressure transducer. The estimated overall accuracy of the pressure coefficient is ±4%, at 20:1 odds.

Mean velocities ($\overline{U}$, $\overline{V}$), turbulent stresses ($\overline{u^2}$, $\overline{uv}$, $\overline{v^2}$) and turbulent triple products ($\overline{u^3}$, $\overline{u^2v}$, $\overline{uv^2}$, $\overline{v^3}$) were measured with a two-component laser Doppler velocimetry (DANTEC 60X FiberFlow LDA) in forward scattered mode. Mist made of light oil was used to seed the wind tunnel. At the measuring volume,



K. KUNOH & Y. SHIRAI

Copyright © 1998, by the International Council of the Aeronautical Sciences (ICAS)
and the American Institute of Aeronautics and Astronautics, Inc.

the fringe spacings are 4.06 and 3.85μm for 514.5 and 488nm laser beam wave length, respectively. The measuring volume is less than 1.2mm in length and 0.1mm in diameter. The Doppler signals from the photomultiplier were processed by two Burst Spectrum Analysers (DANTEC 57N20 BSA). The number of burst samples for each measurement was set at 3000 with a sampling data rate of about 1000Hz. The transit time weighting method[15] was used for the measured data to eliminate velocity bias errors. The estimated overall accuracy is ±4% in mean velocity, ±6% in turbulent stresses, and ±12% in turbulent triple products at 20:1 odds. These values were estimated by taking into account the uncertainties of beam alignment, resolution of the signal processor, and statistical uncertainties. The positioning accuracy of the measuring volume is better than ±0.1mm. Measurements were made for 25 different longitudinal stations between x/h=-2 and 10.

## 3. Experimental Results

Figure 3 shows the surface pressure distributions ($Cp$) plotted against the streamwise directions. Pressure recovery was observed between $x/h = 3$ and 8. Based on this figure and surface oil flow visualisation, it was found that reattachment occurs between $x/h$ =6 and 7.

Distribution of mean velocities, turbulent stresses, and turbulent triple products, which were measured with the LDA, are shown in Figures 4, 5, and 6. A dividing stream line starting from the step, which is defined as a contour of a stream function, $\psi \equiv \int_0^y \overline{U} dy = 0$, is also shown. Streamwise mean velocity profiles (Fig. 4a) show that there is a reverse flow region near the surface. According to Fig. 4a, the reattachment point is at about $x_R/h$ = 6.5. Turbulent stress distribution (Figs. 5a, 5b and 5c) show that after separation, initial growth of the turbulent stress occurs close to the inflection point of the mean longitudinal velocity profile. The level of turbulent intensity decreases after the flow reattaches to the surface. Turbulent triple product distribution (Figs. 6a, 6b, 6c and 6d) is roughly antisymmetric to the centre line of the separated shear layer before reattachment. The overall distributions shown in Figs. 4, 5 and 6 are similar to the previously measured results[5, 8], although the model configuration and the boundary layer condition at the separation are different.

Figure 7 shows a reverse flow rate $R$ plotted against the streamwise direction. Reverse flow rate $R$ is defined as: $R = N_- / N$ , where $N$ denotes the total number of seeded particles that were sampled by BSA, and $N_-$ denotes the number of particles when measured instantaneous longitudinal velocity $U$ is negative. Measurements were made at $y/h$=0.025. A reverse flow rate that is greater than 0.5 means that the reverse is more likely than the forward flow. $R$=0 means that there is no flow reversal. Fig. 7 shows that more than 90% of the particles has reverse velocity between $x/h$ = 2.5 and 4.5. Between the step and $x/h$ = 1, $R$ is less than 0.5. This means that the forward flow is more likely than the reverse flow near the wall at this region. This corresponds to the fact that a secondary separation occurs near the step for the backward-facing step flow[1] that creates a forward flow near the surface of the wall. The streamwise position when $R$=0.5 ($x/h \cong 6.1$) and reattachment point $x_R/h \cong 6.5$, which were obtained in this study, are not the same. This is because the measurements for $R$ were not done at the surface, and that $R$ is defined without taking the velocity of each particle into account.

## 4. Turbulent Energy Balances

In this section, the growth of turbulent stresses will be discussed by using turbulent energy balance equations. The turbulent energy balances and the turbulent normal stress balances were estimated from the transport equations of the turbulent energy ($k$) and turbulent stresses ($\overline{u^2}$, $\overline{v^2}$), in which two-dimensional mean flow and steady turbulence were assumed. The terms were evaluated from the following $k$, $\overline{u^2}$ and $\overline{v^2}$ transport equations.

$$0 = -\left(\overline{U}\frac{\partial k}{\partial x} + \overline{V}\frac{\partial k}{\partial y}\right) - \overline{uv}\left(\frac{\partial \overline{U}}{\partial y} + \frac{\partial \overline{V}}{\partial x}\right) - \left(\overline{u^2}\frac{\partial \overline{U}}{\partial x} + \overline{v^2}\frac{\partial \overline{V}}{\partial y}\right) - \frac{\partial}{\partial x}\overline{uk} - \frac{\partial}{\partial y}\overline{vk} - \varepsilon \quad (1)$$

$$0 = -\left(\overline{U}\frac{\partial}{\partial x} + \overline{V}\frac{\partial}{\partial y}\right)\frac{1}{2}\overline{u^2} - \overline{uv}\frac{\partial \overline{U}}{\partial y} - \overline{u^2}\frac{\partial \overline{U}}{\partial x} - \frac{\partial}{\partial x}\left(\frac{1}{2}\overline{u^3}\right) - \frac{\partial}{\partial y}\left(\frac{1}{2}\overline{u^2 v}\right) - \varepsilon_u + \frac{1}{\rho}\overline{p\frac{\partial u}{\partial x}} \quad (2)$$

$$0 = -\left(\overline{U}\frac{\partial}{\partial x} + \overline{V}\frac{\partial}{\partial y}\right)\frac{1}{2}\overline{v^2} - \overline{uv}\frac{\partial \overline{V}}{\partial x} - \overline{v^2}\frac{\partial \overline{V}}{\partial y} - \frac{\partial}{\partial x}\left(\frac{1}{2}\overline{uv^2}\right) - \frac{\partial}{\partial y}\left(\frac{1}{2}\overline{v^3}\right) - \varepsilon_v + \frac{1}{\rho}\overline{p\frac{\partial v}{\partial y}} \quad (3)$$

Spanwise turbulent stress $\overline{w^2}$ was assumed to be of about the same magnitude as other types of turbulent



K Pinnin & Y. Shima

Copyright © 1998, by the International Council of the Aeronautical Sciences (ICAS)
and the American Institute of Aeronautics and Astronautics, Inc.

stress ($\overline{u^2}$, $\overline{v^2}$) and, therefore, the turbulent energy $k = 1/2 \cdot \left(\overline{u^2} + \overline{v^2} + \overline{w^2}\right)$ can be approximated by $3/4 \cdot \left(\overline{u^2} + \overline{v^2}\right)$. Diffusions by pressure fluctuation $p$ and viscosity were not considered. Dissipation $\varepsilon$ in equation (1) was evaluated as the difference of all the other terms. Estimations of each term were done at every two measured points along the transverse and longitudinal directions. Differentiation was done by using central difference. As for the $\overline{u^2}$ and $\overline{v^2}$ balances, the dissipation ($\varepsilon_u$, $\varepsilon_u$) and the pressure-strain redistribution terms ($\overline{p\partial u/\partial x}/\rho$, $\overline{p\partial v/\partial y}/\rho$) in equations (2) and (3) were not estimated. All terms were made dimensionless by $U_\infty^3/h$.

Figures 8a – 8d show results at several streamwise stations upstream and downstream from the reattachment. Each figure contains balances of turbulent energy $k$ and turbulent normal stress $\overline{u^2}$ and $\overline{v^2}$. Just after separation (Fig.8a, $x/h$=2), the turbulent energy balance shows that production by shear stress $-\overline{uv}(\partial\overline{U}/\partial y + \partial\overline{V}/\partial x)$ is dominant. This term reaches its maximum at the central area of the separated shear layer. The secondary dominant term is dissipation -$\varepsilon$, that was estimated by subtracting the other terms from zero; therefore, there is some scattering. The transverse diffusion $-\partial\overline{vk}/\partial y$ is negative at the central part of the shear layer, and is positive at the outer part as well as near the surface. This means that the turbulent energy that is produced at the centre of the shear layer is transported to the upper and lower areas of the layer by turbulent diffusion. Longitudinal diffusion $-\partial\overline{uk}/\partial x$ is small compared with the transverse one. Production by normal stress $-\overline{u^2}\partial\overline{U}/\partial x - \overline{v^2}\partial\overline{V}/\partial y$ at the centre of the shear layer shows a negative value, which means that energy is transferred to the mean flow by this term. Near the surface, this term is almost zero but has a positive value. Advection $-(\overline{U}\partial k/\partial x + \overline{V}\partial k/\partial y)$ is negative in the upper part of the shear layer. Negative advection implies that the turbulent energy is moved along the stream-line by the mean flow. Near the surface the advection is small but positive. Every term in the reverse flow region near the surface is very small at $x/h$=2.

The $\overline{u^2}$ and $\overline{v^2}$ balances in Fig. 8a show that every term in the $\overline{v^2}$ balance is very small as compared with the $k$ and $\overline{u^2}$ balances. This implies that the growth of $\overline{u^2}$ significantly affects the turbulent energy. The $\overline{v^2}$ production by shear stress $-\overline{uv}\partial\overline{V}/\partial x$ is almost zero in the entire region. The $\overline{v^2}$ production by normal stress $-\overline{v^2}\partial\overline{V}/\partial y$ shows positive values in the central region of the shear layer. On the other hand, $\overline{u^2}$ production by normal stress $-\overline{u^2}\partial\overline{U}/\partial x$ has values that are negative in this region. The fact that the $\overline{v^2}$ production is very small as compared with the $\overline{u^2}$ production but that $\overline{v^2}$ has the same magnitude as $\overline{u^2}$, which was shown in Fig. 5, indicates that the turbulent energy is converted from the longitudinal direction ($x$) to the transverse direction ($y$) due to the pressure-strain redistribution, which was not estimated here.

Examples of balances upstream from the reattachment ($x/h$=4), near the reattachment ($x/h$=6) and downstream from the reattachment ($x/h$=8) are shown in Figs. 8b, 8c and 8d, respectively. The distribution of each term is qualitatively the same as in Fig. 8a. As the shear layer develops and approaches the reattachment, the $y$ position where each term has its peak value moves towards the surface. After reattachment ($x/h$=8), the $k$ production by shear stress has a smaller value than those upstream, which corresponds to the decrease in turbulent stresses that was shown in Fig. 5. The $k$ advection term is positive near the surface in Figs. 8b-8d. Positive advection implies that the turbulent energy is transported into the area along the stream-line by the mean flow. Another difference between Figs. 8b-8d and Fig. 8a is that $k$ production by normal stress does not indicate positive value at $x/h$ = 4, 6 and 8.

4.1 Integrals along a Constant Streamwise Station

The integrals of each term in the turbulent energy balance across the entire measured region at a constant streamwise station are plotted against the streamwise station in Fig. 9a. Each term is made dimensionless by $U_\infty^3$. Again, this shows that the dominant terms in the turbulent energy balance are production by shear stress and dissipation. The transverse diffusion has a value that is almost zero as a consequence of the integrals.

Fig. 9b shows the results obtained by the integration between the surface and the dividing streamline that corresponds to the recirculating region. The distribution of each term is very similar to that in Fig. 9a, except that the advection term is positive near reattachment.

Fig. 9c shows the results that were integrated between the surface and zero velocity line $\overline{U}=0$, which corresponds to the reverse flow region. This shows that not only production by shear stress but also



K. Kiya & T. Sakai

Copyright © 1998, by the International Council of the Aeronautical Sciences (ICAS)
and the American Institute of Aeronautics and Astronautics, Inc.

both the transverse diffusion and the advection similarly help to balance the dissipation. This indicates that the flow within the reverse flow is highly non-equilibrium, i.e. the production and the dissipation are not balanced and that the transverse diffusion and the advection are important in this region.

4.2 Spatial Distribution

Figure 10 shows the spatial distributions of the turbulent energy balance. In this figure, the points where the production by shear stress ($-\overline{uv}(\partial\overline{U}/\partial y+\partial\overline{V}/\partial x)$) reaches its maximum (point A in the diagram) and where the transverse diffusion term ($-\partial\overline{vk}/\partial y$) changes its sign (i.e. zero diffusion points, points B and C) are shown. In order to indicate shear layer growth, the position where the gradient of the mean longitudinal velocity, $\partial\overline{U}/\partial y$, reaches its maximum (point D) and the maximum slope thickness[4], $\delta_\omega$, are indicated. The maximum slope thickness is defined by $\delta_\omega=\overline{U_e}/(\partial\overline{U}/\partial y)_{\max}$, where $\overline{U_e}$ denotes the maximum longitudinal velocity at each streamwise station. Distributions of the $\delta_\omega$ are indicated by ↕ in Fig.10. Maximum slope thickness is a measure of the shear layer growth. In this figure, the dividing streamline and the zero velocity line ($\overline{U}=0$) are also shown.

This figure shows that the streamwise distribution of the maximum production points A and maximum velocity gradient points D are almost similar. The maximum slope thickness distribution shows that the shear layer grows towards the reattachment[2,4]. The turbulent energy is mainly produced within the shear layer. It is also clear that the lower part of zero diffusion point C, the lower part of the maximum slope thickness (↓) and the zero velocity line are located at almost the same position upstream of the reattachment. This implies that shear layer growth is limited within the positive longitudinal velocity area ($\overline{U}>0$). Inside the reverse flow region ($\overline{U}<0$) turbulent transverse diffusion is important, as was shown in Fig. 9.

Figure 11 shows another feature of the spatial distributions of the turbulent energy balance. The points where the advection term in the turbulent energy balance changes its sign ($-(\overline{U}\partial k/\partial x+\overline{V}\partial k/\partial y)$, point E in the diagram) and where the $k$ production by normal stress changes its sign ($-\overline{u^2}\partial\overline{U}/\partial x-\overline{v^2}\partial\overline{V}/\partial y$, point F in the diagram). Just before the reattachment below the $\overline{U}=0$ line, the advection term is positive. This implies that the turbulent energy is transported into the recirculating region from the downstream reattachment area, as was discussed in the previous section. At and below the area where the production by normal stress changes its sign (point F), all of the terms in the turbulent energy balances are very small; therefore, a detailed analysis cannot be made about this area.

Another point G in the diagram is also plotted in this figure. This point G is defined as follows: Figure 12 shows distributions of the $\overline{u^2}$ production term ($-\overline{uv}\partial\overline{U}/\partial y-\overline{u^2}\partial\overline{U}/\partial x$) in equation (2) and the $\overline{v^2}$ production term ($-\overline{uv}\partial\overline{V}/\partial x-\overline{v^2}\partial\overline{V}/\partial y$) in equation (3). Results at $x/h$ = 4, 6 and 8 are shown. These figures show that $\overline{u^2}$ production term is dominant inside the shear layer. However, near the surface, the $\overline{v^2}$ production term is greater than the $\overline{u^2}$ production term upstream from the reattachment (Figs. 12a and 12b). Even negative $\overline{u^2}$ production is observed in this area. The point where $\overline{u^2}$ production is equal to $\overline{v^2}$ production is plotted in Fig. 11 as point G. Near the surface (before reattachment), longitudinal velocity gradient $\partial\overline{U}/\partial y$ is negative due to flow reversal. On the other hand, the sign of measured $\overline{uv}$ did not change near the surface, as was shown in Fig. 5b. This is why negative $\overline{u^2}$ production was observed. The behaviours of the $\overline{v^2}$ production by normal stress, ($-\overline{v^2}\partial\overline{V}/\partial y$), significantly affect the flow near the surface at the reattachment region. Production by shear stress ($-\overline{uv}\partial\overline{V}/\partial x$) is negligible, as was shown in Fig. 8.

4.3 Area Classification

Morinishi and Kobayashi[13] discussed the backward facing flow by numerical simulation. Discussion of the turbulent structure in Ref.13 showed that the separated region could be classified into four distinct regions, i.e. the two types of shear layer region, the near wall region, which is just downstream of the step, and the near wall region near reattachment. Here, a similar analysis was attempted by using the experimental results in this study.

According to the results in Figs. 10 and 11, the turbulent structure of the backward facing step flow can be classified into three regions. Figure 13 shows the region classification. Area 1 in Fig. 13 corresponds to the region just after the separation. Every term of the turbulent energy balance is small. This area corresponds to the region that is often called a "dead air region".



K. RINOIE & Y. SHIRAI

Copyright © 1998, by the International Council of the Aeronautical Sciences (ICAS)
and the American Institute of Aeronautics and Astronautics, Inc.

Area 2 is the region where the transverse diffusion is negative near the surface. Turbulent energy is transported into this region from the upper area. Area 2 can be further classified into three regions: 2A , 2B, and 2C. Area 2A is the region inside the reverse flow and Area 2C is the region that is after the reattachment. Although the mean flow direction is different for two areas, areas 2A and 2C indicate similar characteristics in turbulent energy balances. Area 2B is the area where the $\overline{v^2}$ production term is greater than the $\overline{u^2}$ one as was discussed in Fig.12. In this area, it is a highly non-equilibrium turbulent flow, because not only the production but also the advection and transverse diffusion is dominant, as was shown in Fig. 9 and because $\overline{v^2}$ shows a different type of growth as compared with other areas, as was shown in Fig. 12. Area 3 corresponds to the separated shear layer area that is above zero velocity line. In this area, the flow is similar in behaviour to the plain shear layer.

Classifications of the backward-facing step flow were made from the present results with reference to the results from Ref.13. The measurements in this study indicated the importance of the reattaching area, (i.e. Area2B) in Fig. 13.

## 5. Further Discussion

### 5.1 Shear Layer Growth

In order to understand the behaviours in the shear layer region (Area 3 in Fig.13) in detail, further measurements using an I-type hotwire probe and a constant temperature anemometry were done. Figure 14 shows the power spectral density distributions of longitudinal velocity fluctuations that were measured at different streamwise stations. The transverse hotwire location was set at $y/h$=1.35, which corresponds to the upper part of the shear layer and where the longitudinal mean velocity is almost equal to the freestream velocity. Fig. 14 shows that a dominant peak frequency of 160Hz is observed at $x/h$=3. This dominant frequency gradually shifts towards a lower frequency. Near the reattachment, the dominant frequency is 80Hz, which is half of the value of the initial dominant frequency. The initial frequency of 160Hz is believed to be caused by a similar vortical structure which was found in a two-dimensional plain mixing layer[2]. In this plain mixing layer a "pairing" of the vortical structure occurs. A decrease in the dominant frequency from 160Hz to 80Hz corresponds to this vortex "pairing". In other studies about backward facing step flows[6], the dominant frequency and the vortex "pairing" have been observed. These results in Fig. 14 confirm that the separated shear layer of the backward step has similar characteristics to the two-dimensional mixing layer, as was discussed using the turbulent energy balance. The vortex is caused by the "pairing" that collides at the reattachment point[3]. The behaviour of this vortex near this area might be the reason for the different feature that were observed in area 2B for $\overline{v^2}$ production. However, the turbulent energy balances in the shear layer region (area 3 in Fig. 13) did not indicate any evidence of vortex "pairing".

### 5.2 Generation Process of Reynolds Shear Stress

Wallace and Eckelmann[16] discussed the generation process of the Reynolds stress in the wall region of turbulent boundary layers. It classified the Reynolds stress into four distinct classes of motion. Here, a similar method was used in the backward facing step flow.

Reynolds shear stress $-\overline{uv}$ were classified into four components, (($u$<0, $v$>0), ($u$>0, $v$<0), ($u$>0, $v$>0), ($u$<0, $v$<0)), which will be hereafter referred to as $-\overline{uv_c}$. The four classes of $-\overline{uv_c}$ were estimated from the simultaneously measured instantaneous velocity $U$ and $V$ components. Figure 15 shows the classified Reynolds shear stress distributions together with a net Reynolds stress $-\overline{uv}$ upstream from the reattachment ($x/h$=4, Fig.15a) and downstream from the reattachment ($x/h$=10, Fig.15b). These figures show that the main contributions to $-\overline{uv}$ come from $-\overline{uv_c}$ with ($u$<0, $v$>0) and $-\overline{uv_c}$ with ($u$>0, $v$<0). Two negative contributions of $-\overline{uv_c}$ with ($u$>0, $v$>0) and $-\overline{uv_c}$ with ($u$<0, $v$<0) are almost equal and their magnitude is about one-third of the positive contributions. These tendencies are the same for the turbulent boundary layer results from Ref. 16. In figure 15, the $(\partial \overline{U} / \partial y)_{max}$ location that is close to the centre of the shear layer is indicated. In the upper region of the shear layer both upstream (Fig.15a) and downstream from the reattachment (Fig.15b), positive contributions of $-\overline{uv_c}$ with ($u$<0, $v$>0) are larger than those of $-\overline{uv_c}$ with ($u$>0, $v$<0). This corresponds to the fact that the separated shear layer (as well as the reattached layer) is expanding upwards in this area. After the reattachment, two positive contributions of $-\overline{uv_c}$ near the surface have almost the same magnitude, as are shown in Fig.15b. The positive contributions of $-\overline{uv_c}$ with ($u$>0, $v$<0), however, are larger than those of $-\overline{uv_c}$ with ($u$<0, $v$>0) in the reverse flow region before reattachment (Fig.15a). This might be related to the



K RUNDE & Y SHIRAI

Copyright © 1998, by the International Council of the Aeronautical Sciences (ICAS)
and the American Institute of Aeronautics and Astronautics, Inc.

different behaviour of turbulent normal stress production in the reverse flow region that was discussed in Fig.12.

## 6. Conclusions

Wind tunnel measurements were done for the separated and reattaching flow that was formed over the backward facing step. The turbulent energy and turbulent normal stress balances were estimated from the measured data of mean velocities, Reynolds stresses, and turbulent triple products.

1) The turbulent structure of the backward facing step flow is classified into three regions: the first one is just after separation, where every term of the turbulent energy balance is small (dead air region), the second one is located in the region where the transverse diffusion by turbulence is negative near the surface upstream and downstream of the reattachment, and the third one is the separated shear layer area that is above the zero velocity line. In this area the flow shows similar behaviour to the plain shear layer.

2) The reverse flow region that is upstream of the reattachment is almost identical to the region where the transverse diffusion by turbulence is positive. Here, turbulent energy balances indicate that production by shear stress, the transverse diffusion by turbulence and the advection are similarly involved in balancing dissipation. Just before reattachment, the production of transverse turbulent normal stress in the reverse flow region is larger than that of longitudinal turbulent normal stress.

3) The generation process of the Reynolds stress was discussed by classifying Reynolds stress into four distinct classes of motion. The results indicated that classified Reynolds stresses with $u$ positive and $v$ negative have the most significant effect on Reynolds shear stress in the reverse flow region that is located upstream from the reattachment.

## References

1) Tani, I., Iuchi, M. and Komoda, H., "Experimental Investigation of Flow Separation Associated with a Step or a Groove," Aeronautical Research Institute, Univ. Tokyo, Rep. No.364, April 1961, pp.119-137.

2) Eaton, J.K. and Johnson, J.P., "A Review of Research on Subsonic Turbulent Flow Reattachment," *AIAA Journal*, Vol.19, No.9, 1981, pp.1093-1100.

3) Chandrsuda, C. and Bradshaw, B., "Turbulence Structure of a Reattaching Mixing Layer," *Journal of Fluid Mechanics*, Vol.110, 1981, pp.171-194.

4) Troutt, T.R., Scheelke, B. and Norman, T.R., "Organized structures in a reattaching separated flow field," *Journal of Fluid Mechanics*, Vol.143, 1984, pp.413-427.

5) Driver, D.M. and Seegmiller, H.L., "Features of a Reattaching Turbulent Shear Layer in Divergent Channel Flow," *AIAA Journal*, Vol.23, No.2, 1985, pp.163-171.

6) Driver, D.M., Seegmiller, H.L. and Marvin, J.G., "Time-Dependent Behavior of a Reattaching Shear Layer," *AIAA Journal*, Vol.25, No.7, 1987, pp.914-919.

7) Chiang, S. and Chih-Ming, H., "Three-dimensional Recirculation Flow in a Backward Facing Step," *Journal of Fluids Engineering*, Vol.116, June 1994, pp.228-232.

8) Kasagi, N. and Matsunaga, A., "Three-dimensional Particle-Tracking Velocity Measurement of Turbulence Statistics and Energy Budget in a Backward-Facing Step Flow," *International Journal of Heat and Fluid Flow*, Vol.16, No.6, 1995, pp.477-485.

9) Jovic, S., "An Experimental Study of a Separated/Reattached Flow Behind a Backward-Facing Step. $Re_h$=37,000," NASA TM-110384, April 1996.

10) Patel, V.C., Rodi, W. and Scheuerer, G., "Turbulence Models for Near-Wall and Low Reynolds Number Flows," *AIAA Journal*, Vol.23, No.9, Sep. 1985, pp.1308-1319.

11) Avva, R., Smith, C. and Singhal, A., "Comparative Study of High and Low Reynolds Number Versions of k-e Models," AIAA Paper 90-0246, Jan. 1990.

12) Steffen, C.J., "A Critical Comparison of Several Low Reynolds Number k-$\varepsilon$ Turbulence Models for Flow Over a Backward-Facing Step," AIAA Paper 93-1927, June 1993.

13) Morinishi, Y. and Kobayashi, T., "Turbulence Structure of Separating Region in Backward-Facing Step Flow (Estimation using LES Data)," *Transactions of Japan Soc. Mech. Eng.* Ser.B, Vol.58, No.553, 1992, pp.2730-2735 (in Japanese).

14) Rinoie, K., Saito, Y. and Sunada, Y., "Flow Field Measurements inside the 200mm Width Smoke Wind Tunnel," *Journal of Graduate School and Faculty of Engineering, University of Tokyo*, Ser. B, Vol.44, No.2, 1997, pp.55-63.

15) Petrie, H.L., Samimy, M. and Addy, A.L., "Laser Doppler Velocity Bias in Separated Turbulent Flows," *Experiments in Fluids*, No.6, 1988, pp.80-88.

16) Wallace, J.M., Eckelmann, H. and Brodkey, S., "The Wall Region in Turbulent Shear Flow," *Journal of Fluid Mechanics*, Vol.54, 1972, pp.39-48.



K. RINOIE, Y. SHIRAI

Copyright © 1998, by the International Council of the Aeronautical Sciences (ICAS)
and the American Institute of Aeronautics and Astronautics, Inc.

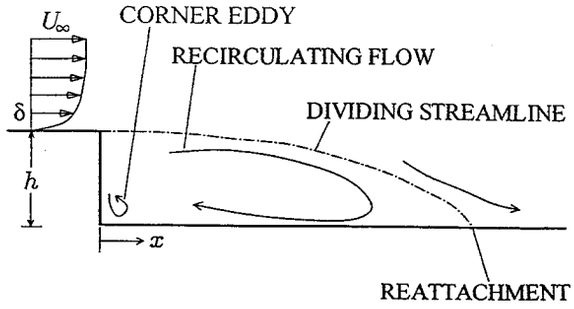


Fig.1 Conceptual sketch of backward-facing step flow.

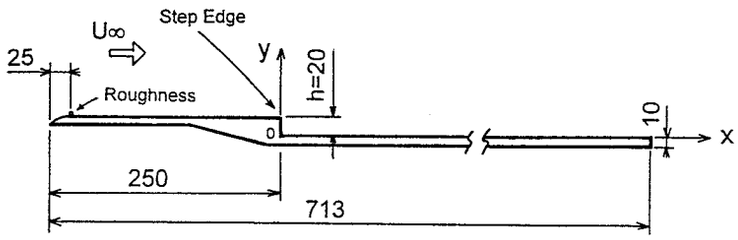


Fig.2 Backward-facing step model.

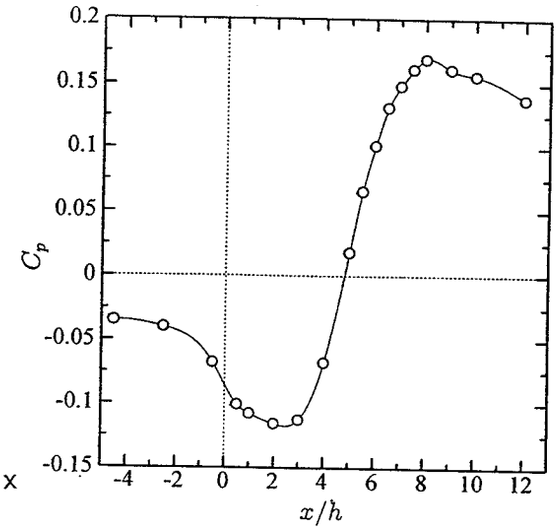


Fig.3 Surface pressure distribution.

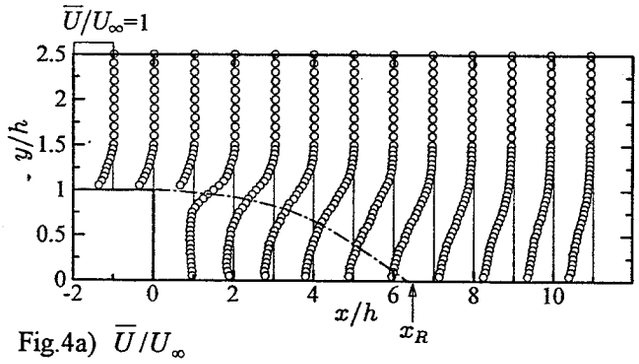


Fig.4a) $\overline{U}/U_\infty$

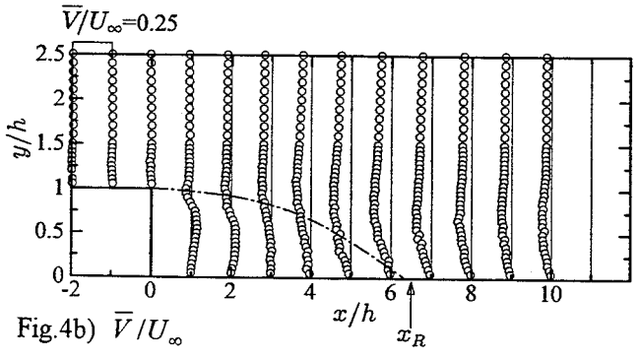


Fig.4b) $\overline{V}/U_\infty$

Fig.4 Mean velocity profiles:

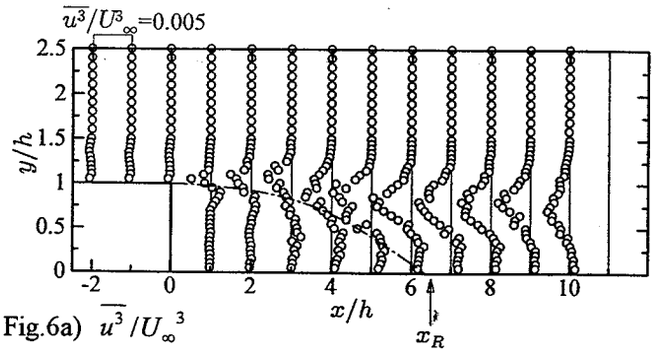


Fig.6a) $\overline{u^3}/U_\infty^3$

Fig.6 Turbulent triple product profiles:

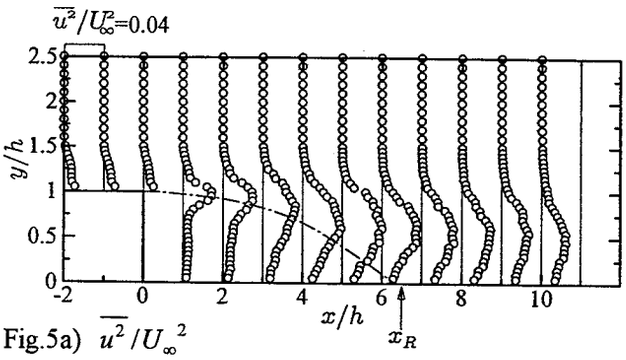


Fig.5a) $\overline{u^2}/U_\infty^2$

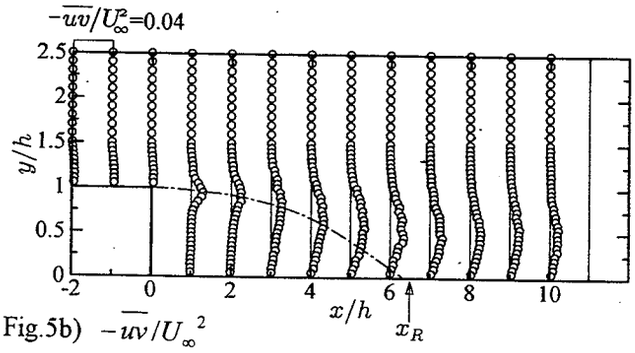


Fig.5b) $-\overline{uv}/U_\infty^2$

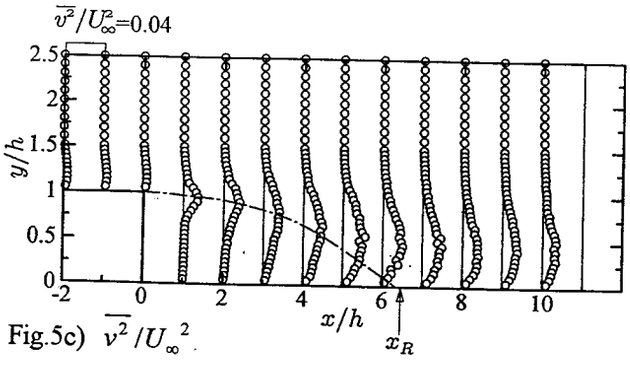


Fig.5c) $\overline{v^2}/U_\infty^2$

Fig.5 Turbulent stress profiles:

K. RINDIE & T. SHIRAI

8/11

Copyright © 1998, by the International Council of the Aeronautical Sciences (ICAS)
and the American Institute of Aeronautics and Astronautics, Inc.

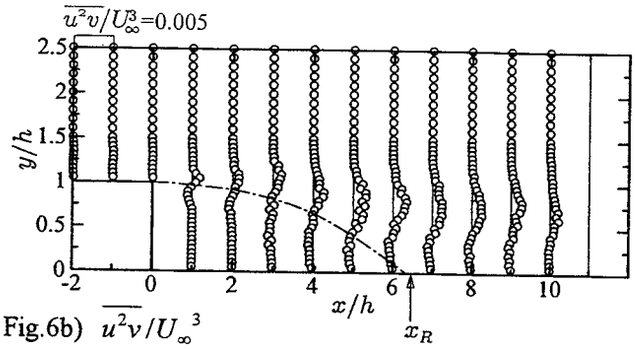


Fig.6b) $\overline{u^2v}/U_\infty^3$

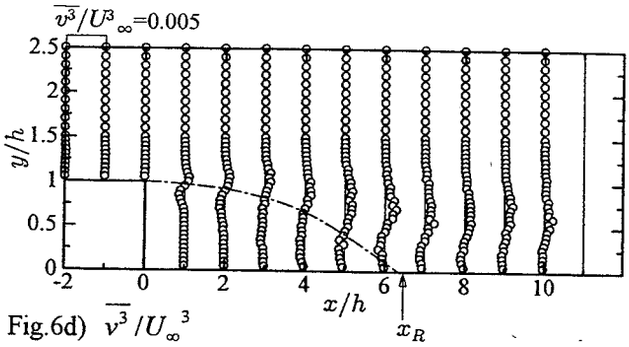


Fig.6d) $\overline{v^3}/U_\infty^3$

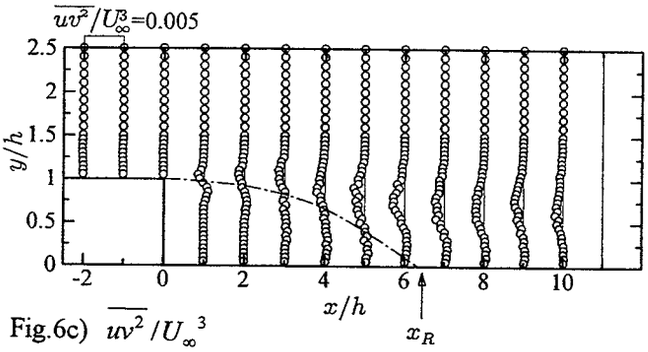


Fig.6c) $\overline{uv^2}/U_\infty^3$

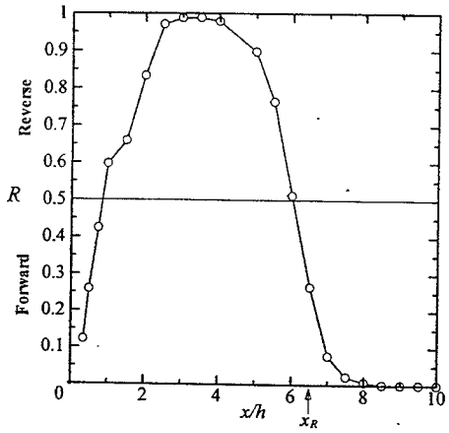


Fig.7 Reverse flow rate distribution.

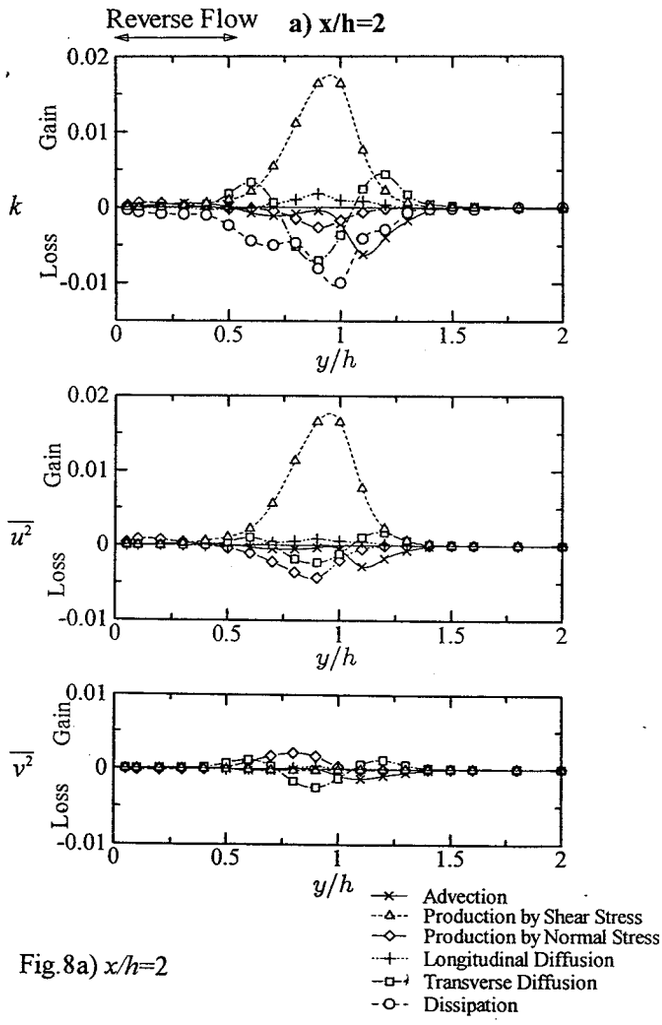


Fig.8a) $x/h$=2

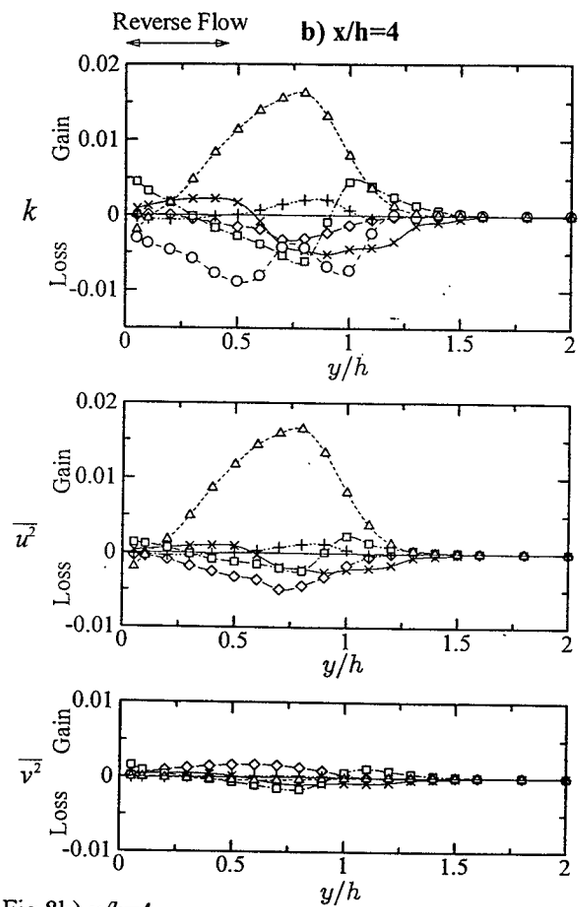


Fig.8b) $x/h$=4

Fig.8 Turbulent energy and turbulent normal stress balances:

K. RINDIE & Y. SHIRAI 9/11

Copyright © 1998, by the International Council of the Aeronautical Sciences (ICAS)
and the American Institute of Aeronautics and Astronautics, Inc.

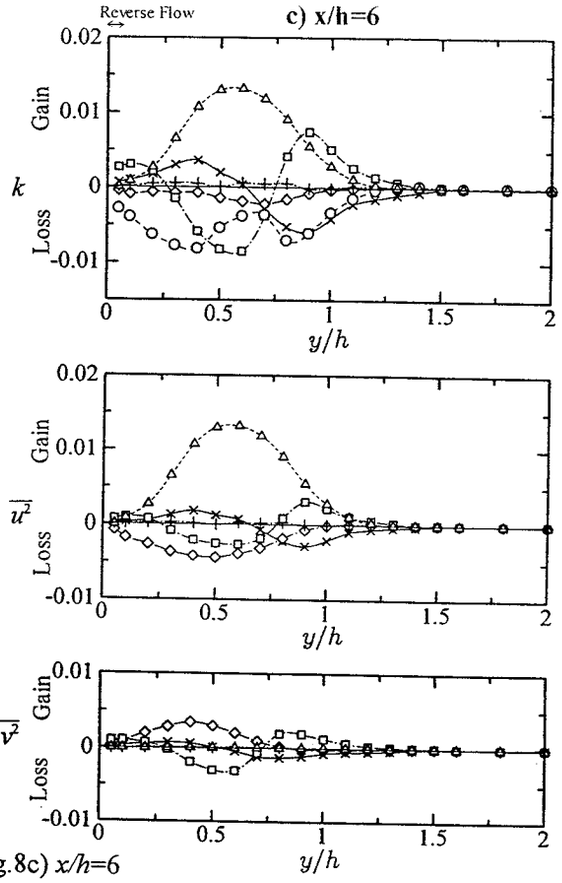


Fig.8c) $x/h$=6

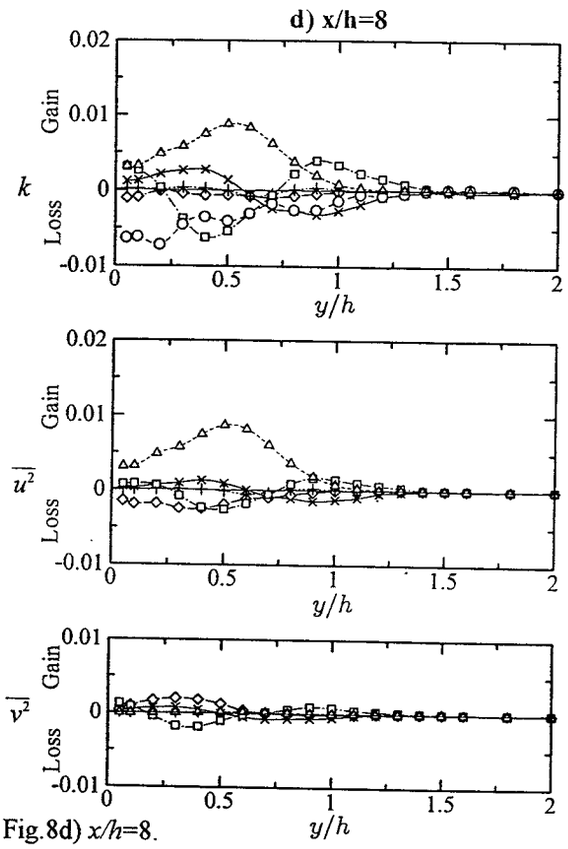


Fig.8d) $x/h$=8.

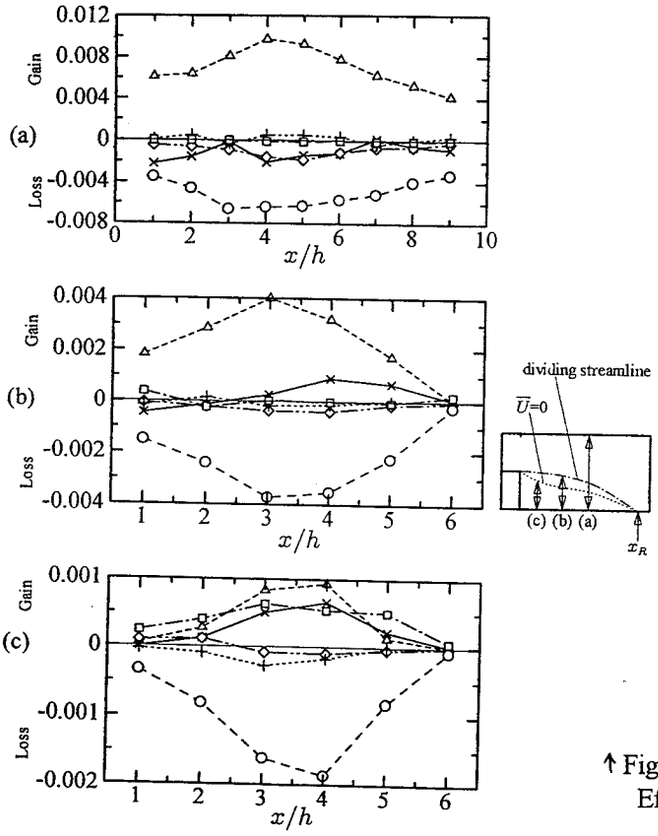


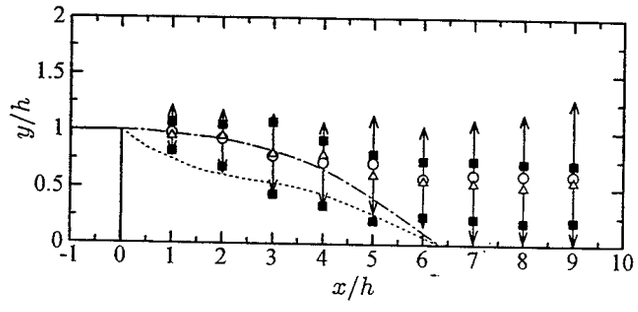


△ Max. k Production by Shear Stress (A)
■ Zero Transverse Diffusion (B, C)
○ $(\partial\overline{U}/\partial y)_{max}$ (D)
↕ Maximum Slope Thickness $\delta_\omega$
Dividing Streamline
$\overline{U}$=0 line

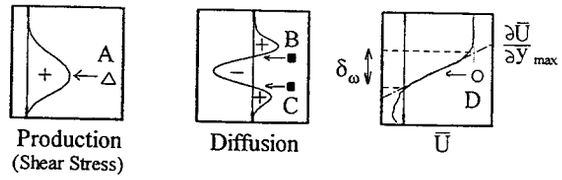


↑ Fig.10 Spatial distribution of turbulent energy balance (1): Effects of production by shear stress and transverse diffusion.

- Advection
- Production by Shear Stress
- Production by Normal Stress
- Longitudinal Diffusion
- Transverse Diffusion
- Dissipation

← Fig.9 Integrals of turbulent energy balances:
a) integrals across an entire layer
b) integrals below the dividing streamline
c) integrals within the reverse flow.



K. RINOIE & Y. SHIRAI

Copyright © 1998, by the International Council of the Aeronautical Sciences (ICAS)
and the American Institute of Aeronautics and Astronautics, Inc.

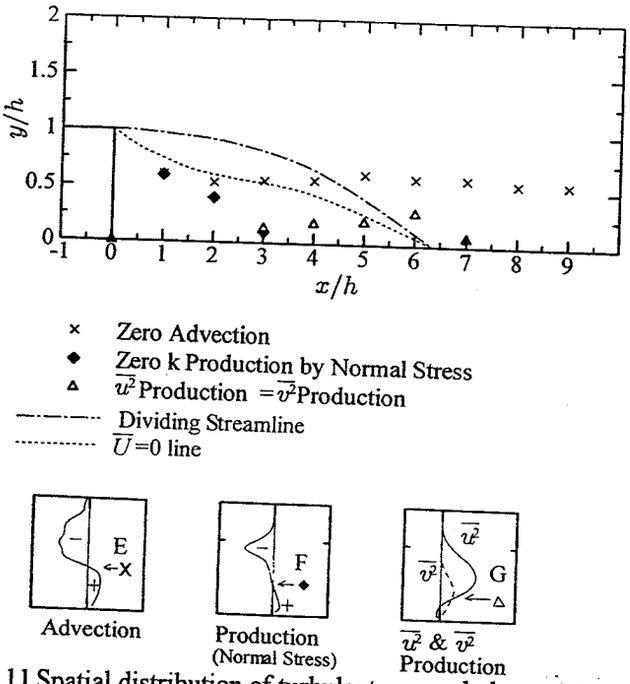


Fig.11 Spatial distribution of turbulent energy balance (2): Effects of advection, production by normal stress and $\overline{u^2}$, $\overline{v^2}$ production.

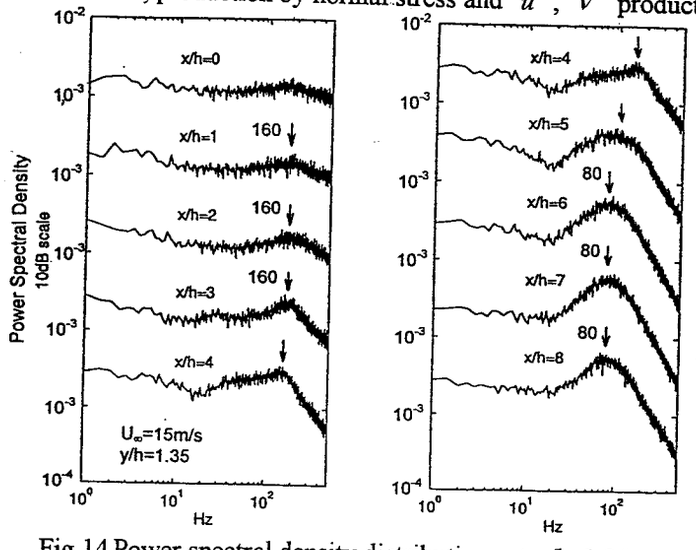


Fig.14 Power spectral density distributions at $y/h$=1.35.

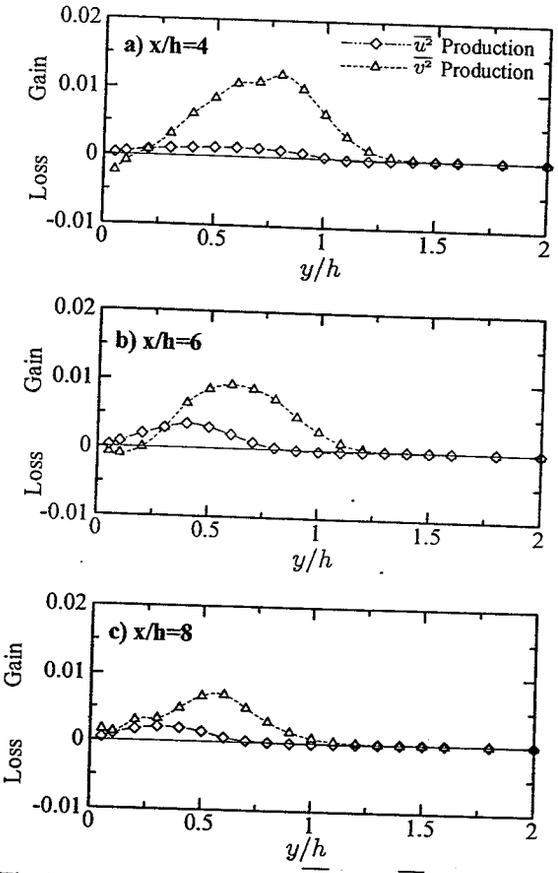


Fig.12 Production terms in $\overline{u^2}$ and $\overline{v^2}$ equations.

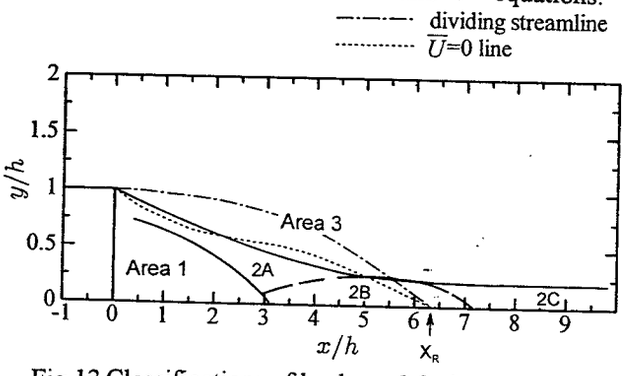


Fig.13 Classifications of backward-facing step flow.

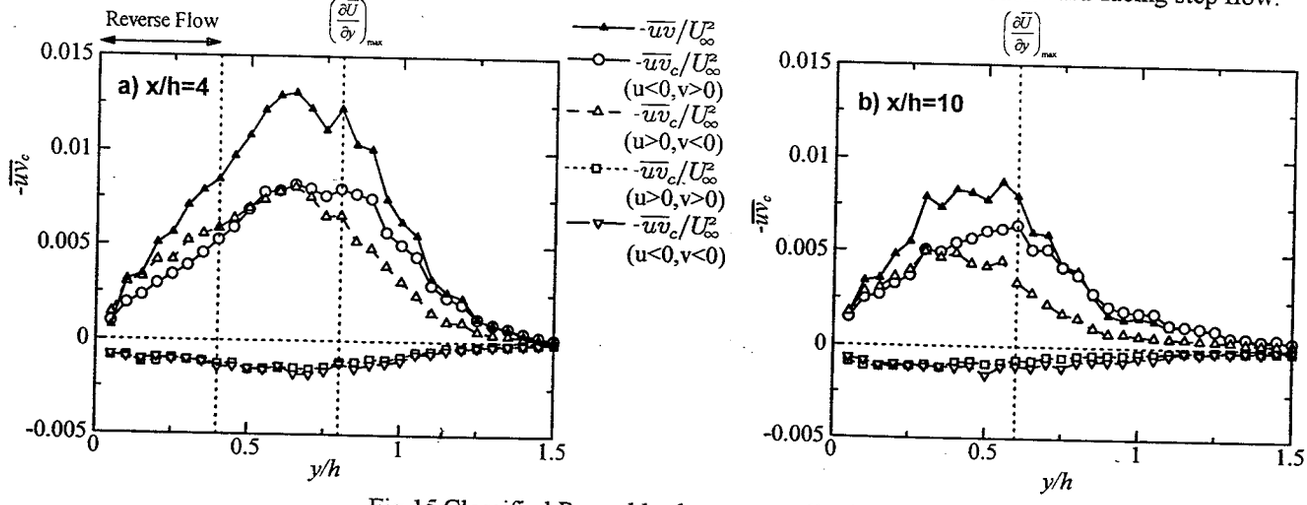


Fig.15 Classified Reynolds shear stress distribution.



K. RINOIE & Y. SHIRAI